Journal of Materials Chemistry A

COMMUNICATION

View Article Online
View Journal | View Issue

Cite this: J. Mater. Chem. A, 2016, 4, 1174

Received 26th October 2015
Accepted 27th November 2015

DOI: 10.1039/c5ta08593d

www.rsc.org/MaterialsA

A novel polysulfone–polyvinylpyrrolidone membrane with superior proton-to-vanadium ion selectivity for vanadium redox flow batteries†

Chunxiao Wu, Shanfu Lu,* Haining Wang, Xin Xu, Sikan Peng, Qinglong Tan and Yan Xiang*

A novel kind of effective vanadium ion-suppressed polysulfone–polyvinylpyrrolidone (PSF–PVP) membrane with high ion selectivity, superior stability and low cost is designed and constructed for vanadium redox flow batteries (VRFBs). The VRFB with the PSF–PVP–50 membrane exhibits impressive coulombic efficiency (98%) as well as energy efficiency (89%), and outstanding stability during the 2000 h continuous charge–discharge cycling test.

Reliable energy storage technology utilized for grid-scale applications is necessary to mitigate environmental and energy issues that have received wide attention.[1–4] Vanadium redox flow batteries (VRFBs), invented by Skyllas-Kazacos in 1985,[5] are leading the way to address this issue due to their pollution-free operation, life-term stability, high energy efficiency, and flexible power supply design.[6–9] As a key component of the VRFB, ion exchange membranes (IEMs) are used to separate the cathode and anode electrolyte, while still permitting the transfer of protons. Therefore, IEMs with high proton conductivity, low vanadium ion permeability, and high chemical stability are critical to improving battery performance. The commercial membrane, Nafion®, is commonly chosen for VRFBs due to its high conductivity and excellent chemical stability. However, the commercialization of VRFB is hindered by the serious vanadium ion permeability and high cost of Nafion®.[10–19] Surface or bulk modification of Nafion® has been proposed to suppress the vanadium ion permeability yet it usually causes a decrease in proton conductivity. Another method is to develop an alternative membrane such as cation exchange membranes,[20–22] nanofiltration membranes[23] and anion exchange membranes.[24–26] However, it is still a critical challenge to balance the proton conductivity and vanadium ion permeability in order to obtain high ion selectivity.

Beijing Key Laboratory of Bio-inspired Energy Materials and Devices, School of Chemistry and Environment, Beihang University, Beijing, 100191, P. R. China. E-mail: lusf@buaa.edu.cn; xiangy@buaa.edu.cn

† Electronic supplementary information (ESI) available. See DOI: 10.1039/c5ta08593d

Polyvinylpyrrolidone (PVP) (Fig. S1 in the ESI†) is a typical hydrophilic polymer that has been widely used to prepare phase inverse membranes[27] and nanofiltration membranes.[28] Recently, we reported that PVP was used to fabricate composite proton exchange membranes with high conductivity since the nitrogen heterocycle of PVP is capable of accepting protons from inorganic acids, such as phosphoric acid[29,30] or phosphotungstic acid.[31]

Herein, a novel polysulfone–polyvinylpyrrolidone homogenous membrane with superior proton-to-vanadium ion selectivity and chemical stability for VRFB applications is successfully constructed through a simple polymer blending method. The performance of as-prepared membranes (denoted as PSF–PVP–*x*, where *x* stands for the weight percentage of PVP in the membrane) could be modulated by the content of PVP. When the PVP content is 50 wt% and the membrane thickness is 35 μm, a superior proton-to-vanadium ion selectivity of 288 times higher than that of Nafion 212 is achieved. The excellent ion selectivity benefits from the electrostatic repulsion of protonated PVP molecules and the smaller ion transfer channels than Nafion. Furthermore, PSF–PVP–*x* membranes possess superior anti-oxidation stability during 400 days of testing of the membrane exposed to the VO_2^+/H_2SO_4 electrolyte. More importantly, the VRFB based on PSF–PVP–50 with 35 μm thickness exhibits an impressive coulombic efficiency of 98% as well as an energy efficiency of 89% with high stability during the 2000 h charge–discharge cycling test. The electrochemical performance of the PSF–PVP membranes combined with a facile fabrication process and cost-effective raw materials promote its commercial application in the vanadium redox flow battery industry.

The PSF–PVP–*x* membrane was prepared through a simple polymer solution casting method (see the detailed process in the Experimental section of the ESI†). Fig. 1a and b show a typical photograph and cross-sectional scanning electron microscopy (SEM) image of the as-prepared the PSF–PVP–*x*. The photograph (Fig. 1a) shows that the PSF–PVP–*x* membrane is homogeneous, transparent and flexible. As shown in Fig. 1b and

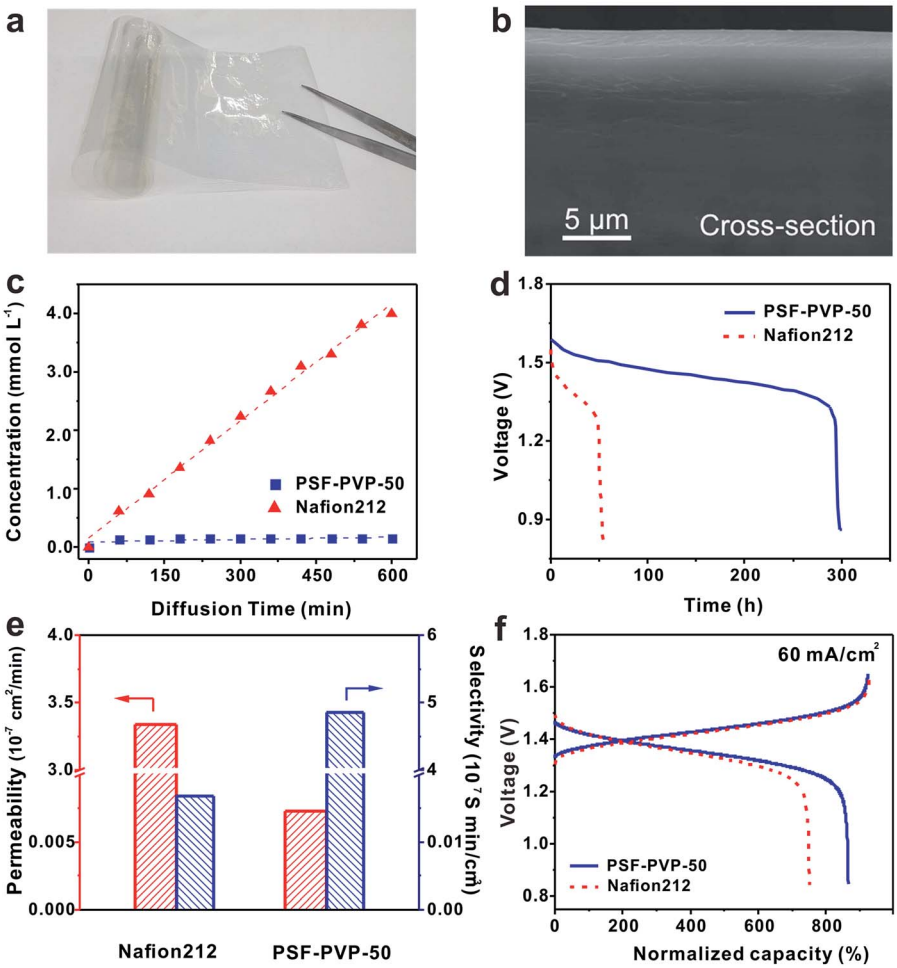

Fig. 1 (a) Photograph and (b) SEM cross-sectional image of the PSF–PVP homogenous membrane. The PSF–PVP–*x* membrane is transparent, homogenous, flexible and dense without porosity on a microscale. (c) The diffusion rate of vanadium ions in the PSF–PVP–50 membrane compared with that of Nafion 212. (d) The plots of open circuit voltage over time for VRFB with PSF–PVP–50 and Nafion 212 respectively. (e) Vanadium permeability and ion selectivity of the PSF–PVP–50 membrane compared with that of Nafion 212. The PSF–PVP–50 membrane exhibits a lower diffusion rate of vanadium ions and higher selectivity than that of Nafion 212. (f) Charge–discharge curves of VRFBs. The one with PSF–PVP–50 shows improved performance compared that with Nafion 212.

S2 in the ESI,† the cross-sectional and surface morphologies indicate that the membrane is dense and without any porous structures. Furthermore, all of the PSF–PVP–*x* membranes possess satisfactory mechanical strength (up to 50 MPa) as well as excellent dimensional stability in vanadium ion electrolyte solution (Table S1 in the ESI†), which permits the fabrication of a thin membrane for practical applications.

The vanadium ion permeability of PSF–PVP–*x* membranes was determined by a diffusion cell method. The linear relationship between the concentration and diffusion time of VO^{2+} ions for both Nafion 212 and PSF–PVP–50 membranes is shown in Fig. 1c. The diffusion rate of vanadium ions with the PSF–PVP–50 membrane is 1/314 of that in Nafion 212 according to the slope, even the thickness of PSF–PVP–50 (~35 μm) is 70% of Nafion 212 (~51 μm). As a result, the VRFB with the PSF–PVP–50 membrane will exhibits a much lower self-discharge rate. The single battery with the PSF–PVP–50 membrane maintains an open circuit voltage (OCV) above 1.3 V for more than 290 h (Fig. 1d), which is above 6 times higher than that with Nafion 212 (45 h) under the same conditions. Even though the proton conductivity of PSF–PVP–50 is 36 mS cm^{-1} which is slightly lower than that of Nafion 212 (56 mS cm^{-1}), the vanadium ion permeability is much lower; as a result, the proton-over-vanadium ion selectivity is 282 times higher than that of Nafion 212 (Fig. 1e). Therefore, VRFBs with the PSF–PVP–50 membrane demonstrate a larger discharge capacity (under the same normalized charge capacity) and similar voltage platforms in comparison to that with Nafion 212 (Fig. 1f), indicating a higher coulombic efficiency (discharge-over-charge capacity).

In the PSF–PVP membranes, PSF acts as a skeleton to improve the formation and mechanical strength of the membrane, and PVP as the typical hydrophilic polymer with a nitrogen heterocyclic structure plays a very important role in the membrane properties (such as the vanadium ion suppression and proton conductivity) due to its hydrophilicity and protonation ability. With the increase of PVP content, PSF–PVP

membranes exhibit substantially enhanced hydrophilicity (Fig. S2 in the ESI†), water uptake and swelling degree (Table S1, ESI†). More importantly, with the decrease of PVP content from 70% to 40% in the membrane, the proton conductivity gradually reduces from 38.2 to 22.7 mS cm^{-1} with a decrease of 40.6% (Fig. 2a), meanwhile the VO^{2+} ion permeability sharply reduces from 0.05×10^{-7} to 0.003×10^{-7} cm^2 min^{-1} with a decrease of 93% (Fig. 2b). As a result, the ion selectivity of PSF–PVP–*x* significantly is enhanced from 0.81×10^7 to 6.7×10^7 S min cm^{-3} with the decrease of PVP content from 70 wt% to 40 wt%. In particular, the PSF–PVP–40 and PSF–PVP–50 membranes have an extremely high ion selectivity of 6.7×10^7 and 4.8×10^7 S min cm^{-3} respectively, which is 394 and 282 times higher than that of Nafion 212 (0.017×10^7 S min cm^{-3}) (Table S1, ESI†). Considering the area resistance and vanadium permeability, PSF–PVP–50 is the most appropriate membrane for VRFB applications.

In order to illustrate the extremely low vanadium ion permeability of PSF–PVP membranes, the zeta potential of pure PVP dissolved in H_2O or H_2SO_4 solution was measured. As shown in Fig. 2c, the zeta potential of the PVP molecule in H_2O is −1.1 mV and changes to 236 mV in 0.005 M H_2SO_4 solution, which demonstrates that PVP molecules could be protonated in acidic solution due to the N-heterocyclic groups in the side chains. This result suggests that the PSF–PVP membrane could produce natural barriers and strongly prevent the crossover of vanadium ions due to the electrostatic repulsion.[32–34] Furthermore, the transmission electron microscopy (TEM) characterization was carried out to have an insight into the ion transfer channels inside the membrane. The ion transfer channels could be represented and labeled by iodine nanoparticles (I_2 NPs) formed by iodine molecules reacting with PVP in the PSF–PVP membrane.[35] As shown in Fig. 2d, the dark zones (I_2 NPs) in the TEM image indicate that the channels are uniformly distributed in the membrane with size of around 2 nm, which is much smaller than that of Nafion® (~4 nm).[3] In addition, with an increase of PVP content in the membrane, the number of ion channels correspondingly increases and the size of channels is almost constant (Fig. S4 in the ESI†). Due to the limited size of hydrophilic channels and the exclusive effect by the protonated PVP, the hydro protons are much easier to transfer across the charged membrane than hydrated vanadium ions.[2] However, the vanadium ion permeability still increases as the PVP content increases because the N-heterocyclic groups in unit volume decreases due to the large swelling ratio (as shown in Fig. S5 in the ESI†). The possible ion transfer pathway inside the membrane is shown in Fig. 2e.

VRFBs with PSF–PVP membranes of varied PVP contents show different voltage platforms and charge–discharge capacities under current densities of 30–60 mA cm^{-2} (Fig. 3a and S6 in the ESI†). The VRFB with PSF–PVP–40 exhibits the highest charge platform and lowest discharge platform due to the largest resistance, even with the lowest vanadium ion permeability. Meanwhile, the VRFB with PSF–PVP–60 holds the lowest

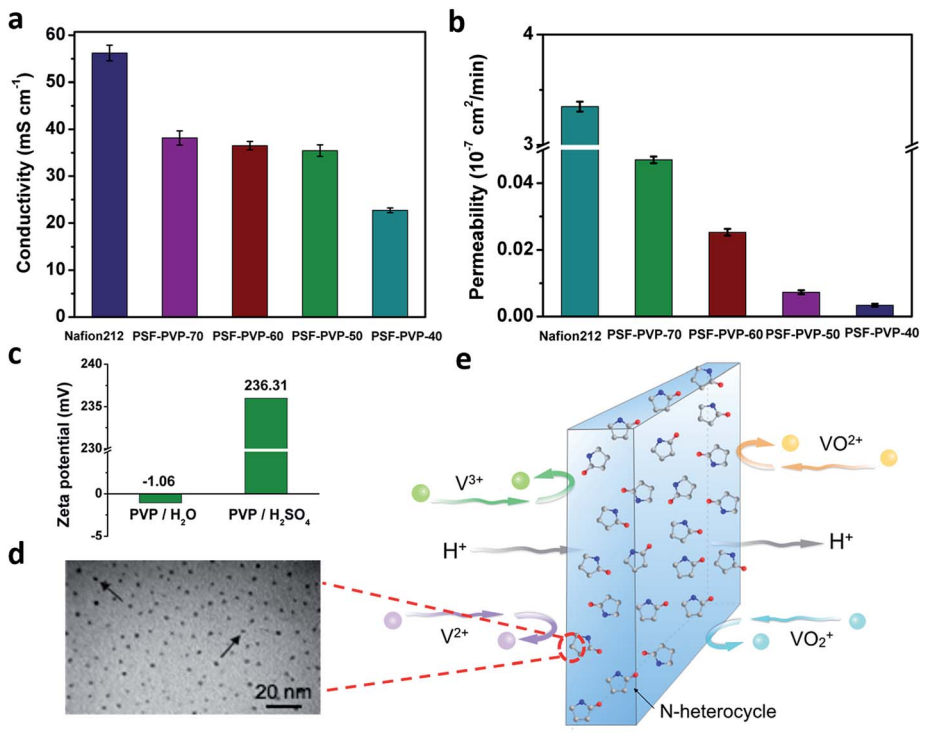

Fig. 2 (a) Proton conductivity and (b) VO^{2+} ion permeability of the PSF–PVP–*x* membranes, in comparison with Nafion 212. (c) Zeta potential of pure PVP dissolved in 0.005 M H_2SO_4 solution and H_2O respectively. (d) Transmission electron microscopy (TEM) image of the PSF–PVP–50 membrane after being stained with iodine vapour. The dark zones (I_2 nanoparticles) indicate the size of hydrophilic channels of around 2 nm. (e) The schematic of the proposed mechanism for proton transfer and vanadium ion suppression of the PSF–PVP–*x* membrane.

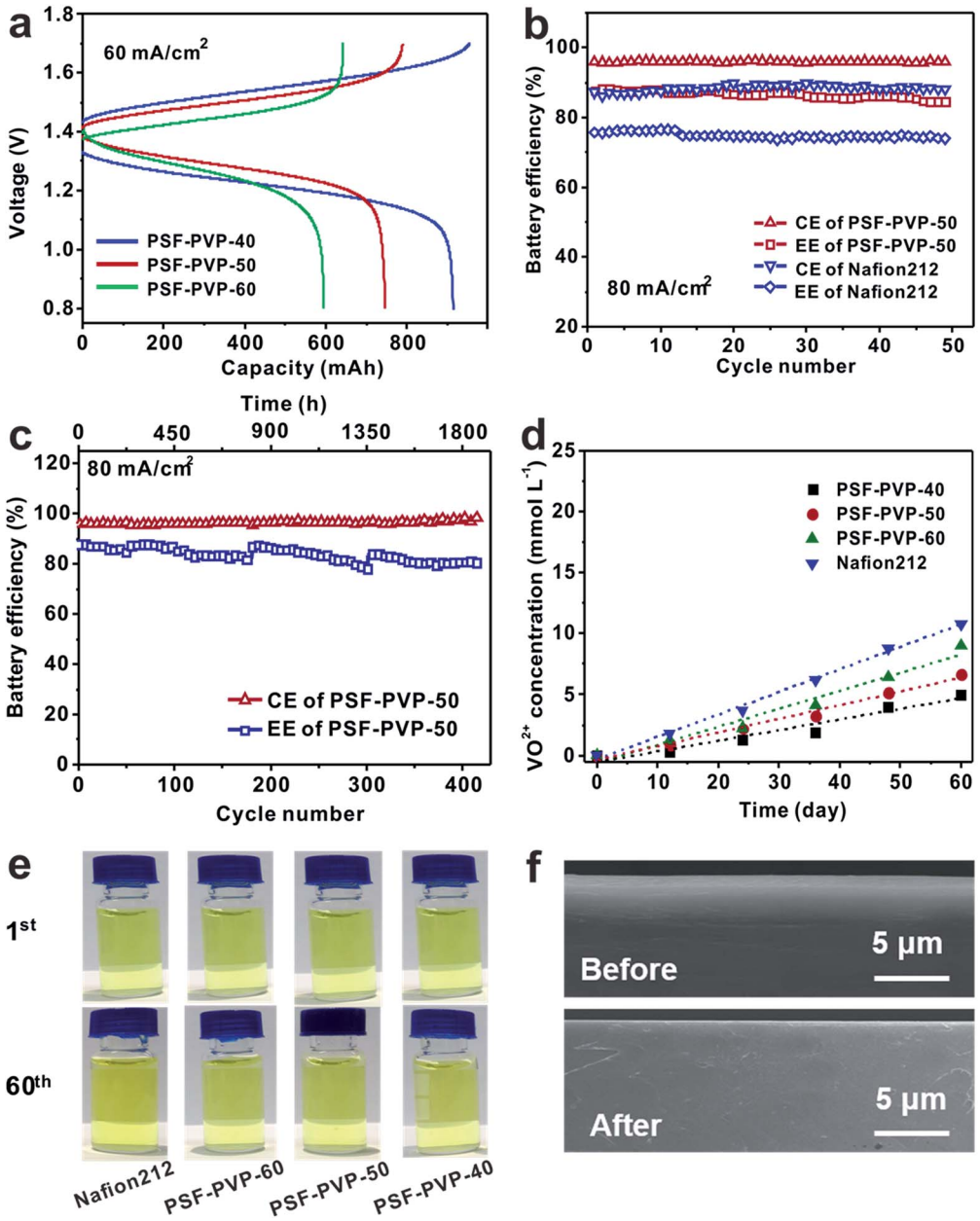

Fig. 3 (a) Charge–discharge curves of VRFBs with PSF–PVP–*x* membranes. (b) Coulombic efficiency (CE) and energy efficiency (EE) of the PSF–PVP–*x* battery compared with Nafion 212 and (c) cyclic stability of the PSF–PVP–50 battery. (d) Chemical stability of PSF–PVP–*x* membranes compared with Nafion 212. (e) After 60 days of the anti-oxidant test, the color of the VO_2^+ solution has almost no change and (f) cross-sectional SEM image of the membrane before and after immersion in VO_2^+ solution for 400 days. According to the charge–discharge curves, PSF–PVP–50 membranes exhibit optimal performance relative to others and Nafion 212, the VRFB with PSF–PVP–50 exhibits superior stability and higher coulombic efficiency and energy efficiency.

charge platform due to the lowest resistance, however the high vanadium ion permeability results in a lower discharge platform and the lowest discharge capacity. Therefore, the energy efficiency (EE) is a more reasonable parameter to evaluate the VRFB performance. As shown in Table S2 in the ESI,† the VRFB with PSF–PVP–50 membrane shows a high coulombic efficiency (CE) of 97% and voltage efficiency (VE) of 88%, and achieved the best EE of 85% under a charge–discharge current density of 60 mA cm^{-2}. Furthermore, the membrane thickness is another critical parameter for the EE of VRFB. As shown in Table S3 and Fig. S7 in the ESI,† the VRFB exhibits optimal EE when the membrane thickness is 35 μm. Meanwhile, the optimal VRFB displays a higher CE and EE than that with Nafion 212 over the duration of a 50-cycle test at different current densities (Fig. 3b and S8 in the ESI†). In comparison with previous studies (listed in Table 1), VRFBs with the PSF–PVP–50 membrane exhibits a higher CE and EE than those with sulfonated polyether ether ketone (SPEEK),[12] chloromethylated polysulfone (CPSF)[2] or polyvinylidenefluoride (PVDF)[23] membranes, *etc.* Additionally, the VRFB with the PSF–PVP–50 membrane shows adequate

Table 1 The performances of VRFBs with PSF–PVP–50 in comparison with previous work

	Thickness (μm)	CE (%)	EE (%)	VE (%)	I (mA cm^{-2})	OCV (h)	Ref.
CPSF-Py	250	96	87	91	80	NA	2
Nafion/PEI	208	97	81	83	50	265	10
Porous PVDF	155	96	80	83	60	70	23
SPEEK	90	96	87	90	60	160	12
Nafion 212	51	92	79	86	80	40	18
PSF–PVP–50	35 ± 2	98	90	91	80	289	This study

performance even under a large charge–discharge current density of 80–120 mA cm^{-2} (Fig. S9 in the ESI†) with a CE around 95% and EE of around 80%, which ensures that the PSF–PVP–50 membranes and the PVP–50 membrane could be applied within a large current density range and meet the need of unstable energy storage.[36] More importantly, this merit would be great help for the small size device design as well as for reducing the device cost.

In order to evaluate the life-time stability of the PSF–PVP–50 membrane in VRFBs, over 400 charge–discharge cycles tests were carried out under a current density of 80 mA cm^{-2}, as shown in Fig. 3c. During continuous running for nearly 2000 hours, the battery exhibits the CE of ~98% and EE of ~89% without obvious decay (the fluctuation of EE is caused by the replacement of the electrolyte). The excellent anti-oxidant stability of the PSF–PVP–x membranes may provide an important contribution to the outstanding life-term stability of the battery. Most polymeric membranes decompose or oxidize in VRFBs due to the strong oxidization of VO_2^+ and acidity of H_2SO_4.[37–39] Thus, the chemical stability of PSF–PVP–x membranes is evaluated by the anti-oxidant tests in VO_2^+ solution for a duration of 60 days in comparison with that of Nafion 212. UV-vis analysis was employed to evaluate the generation rate of VO^{2+} ions as reduced from VO_2^+. As shown in Fig. 3d, the generation rate of VO^{2+} ions for PSF–PVP membranes is less than 5×10^{-6} mmol L^{-1} h^{-1}, which is lower than that of Nafion 212 (7.6×10^{-6} mmol L^{-1} h^{-1}). After 60 days, the color of the VO_2^+ solution shows almost no change (Fig. 3e). Furthermore, the SEM cross-sectional image of PSF–PVP soaked in 1 M VO_2^+/3 M H_2SO_4 solutions for about 400 days is still dense without any obvious porosity changes (Fig. 3f). Additionally, the results of the gel permeation chromatography test indicate that the molecular weight of PVP and PSF in the membrane does not show obvious change after the PSF–PVP membrane was soaked in VO_2^+/H_2SO_4 solutions for 400 days (Fig. S10 in the ESI†). All results clearly reveal that PSF–PVP membranes have superior chemical stability under the operating conditions of VRFBs.

Conclusions

In summary, novel PSF–PVP homogenous membranes with superior proton-over-vanadium ion selectivity, satisfactory mechanical strength and excellent chemistry stability are designed with cheap raw materials and a simple fabrication process for VRFB applications. The superior ion selectivity of PSF–PVP membranes was attributed to the electrostatic repulsion effect and the limited ion transfer channels. Impressive coulombic efficiency (98%) and energy efficiency (89%) are achieved in a single VRFB with the PSF–PVP–50 membrane, even in a large current density range. More specifically, it is accompanied by superior life-term stability for retaining the high efficiencies over the duration of the 2000 h charge–discharge test. The PSF–PVP membranes with outstanding performance and low cost can be considered as the promising materials for commercial VRFB applications.

Acknowledgements

This work was financially supported by grants from the National Natural Science Foundation of China (No. 21576007, 51422301, U1137602), National High Technology Research and Development Program of China (863 program, 2013AA031902), and Beijing Higher Education Young Elite Teacher Project (No. 29201493).

Notes and references

1 Z. Yang, J. Zhang, M. C. Kintner-Meyer, X. Lu, D. Choi, J. P. Lemmon and J. Liu, *Chem. Rev.*, 2011, **111**, 3577–3613.
2 H. Zhang, H. Zhang, F. Zhang, X. Li, Y. Li and I. Vankelecom, *Energy Environ. Sci.*, 2013, **6**, 776.
3 J. Brodd and M. Winter, *Chem. Rev.*, 2004, **104**, 4245–4269.
4 C. Liu, F. Li, L. P. Ma and H. M. Cheng, *Adv. Mater.*, 2010, **22**, E28–E62.
5 E. Sum and M. Skyllas-Kazacos, *J. Power Sources*, 1985, **15**, 179–190.
6 M. Skyllas-Kazacos, M. Chakrabarti, S. Hajimolana, F. Mjalli and M. Saleem, *J. Electrochem. Soc.*, 2011, **158**, R55–R79.
7 Z. Yang, J. Zhang, M. C. Kintner-Meyer, X. Lu, D. Choi, J. P. Lemmon and J. Liu, *Chem. Rev.*, 2011, **111**, 3577–3613.
8 H. Zhang, H. Zhang, X. Li, Z. Mai and J. Zhang, *Energy Environ. Sci.*, 2011, **4**, 1676–1679.
9 X. Wei, Z. Nie, Q. Luo, B. Li, B. Chen, K. Simmons, V. Sprenkle and W. Wang, *Adv. Energy Mater.*, 2013, **3**, 1215–1220.
10 Q. Luo, H. Zhang, J. Chen, P. Qian and Y. Zhai, *J. Membr. Sci.*, 2008, **311**, 98–103.
11 B. Schwenzer, J. Zhang, S. Kim, L. Li, J. Liu and Z. Yang, *ChemSusChem*, 2011, **4**, 1388–1406.

12 Z. Mai, H. Zhang, X. Li, C. Bi and H. Dai, *J. Power Sources*, 2011, **196**, 482–487.
13 H. Vafiadis and M. Skyllas-Kazacos, *J. Membr. Sci.*, 2006, **279**, 394–402.
14 G. Hu, Y. Wang, J. Ma, J. Qiu, J. Peng, J. Li and M. Zhai, *J. Membr. Sci.*, 2012, **407**, 184–192.
15 S. Zhang, C. Yin, D. Xing, D. Yang and X. Jian, *J. Membr. Sci.*, 2010, **363**, 243–249.
16 W. Wei, H. Zhang, X. Li, Z. Mai and H. Zhang, *J. Power Sources*, 2012, **208**, 421–425.
17 F. Zhang, H. Zhang and C. Qu, *ChemSusChem*, 2013, **6**, 2290–2298.
18 F. Zhang, H. Zhang and C. Qu, *J. Phys. Chem. B*, 2012, **116**, 9016–9022.
19 S. Lu, C. Wu, D. Liang, Q. Tan and Y. Xiang, *RSC Adv.*, 2014, **4**, 24831–24837.
20 Z. Li, W. Dai, L. Yu, J. Xi, X. Qiu and L. Chen, *J. Power Sources*, 2014, **257**, 221–229.
21 W. Wang, Q. Luo, B. Li, X. Wei, L. Li and Z. Yang, *Adv. Funct. Mater.*, 2013, **23**, 970–986.
22 J. Li, Y. Zhang, S. Zhang and X. Huang, *J. Membr. Sci.*, 2015, **490**, 179–189.
23 J. Cao, H. Zhang, W. Xu and X. Li, *J. Power Sources*, 2014, **249**, 84–91.
24 B. Yin, Z. Li, W. Dai, L. Wang, L. Yu and J. Xi, *J. Power Sources*, 2015, **285**, 109–118.
25 S. Yun, J. Parrondo and V. Ramani, *J. Mater. Chem. A*, 2014, 1–3.
26 Z. Yuan, X. Li, Y. Duan, Y. Zhao and H. Zhang, *J. Membr. Sci.*, 2015, **488**, 194–202.
27 M. J. Han and S. T. Nam, *J. Membr. Sci.*, 2002, **202**, 55–61.
28 S. H. Yoo, J. H. Kim, J. Y. Jho, J. Won and Y. S. Kang, *J. Membr. Sci.*, 2004, **236**, 203–207.
29 Z. Guo, X. Xu, Y. Xiang, S. Lu and S. P. Jiang, *J. Mater. Chem. A*, 2015, **3**, 148–155.
30 X. Xu, H. Wang, S. Lu, Z. Guo, S. Rao, R. Xiu and Y. Xiang, *J. Power Sources*, 2015, **286**, 458–463.
31 S. Lu, X. Xu, J. Zhang, S. Peng, D. Liang, H. Wang and Y. Xiang, *Adv. Energy Mater.*, 2014, **140**, 842.
32 L. M. Vane and G. M. Zang, *J. Hazard. Mater.*, 1997, **55**, 1–22.
33 X. Li, H. Zhang, Z. Mai, H. Zhang and I. Vankelecom, *Energy Environ. Sci.*, 2011, **4**, 1147.
34 S. Kim, T. B. Tighe, B. Schwenzer, J. Yan, J. Zhang, J. Liu, Z. Yang and M. A. Hickner, *J. Appl. Electrochem.*, 2011, **41**, 1201–1213.
35 J. Wu, P. Li, S. Hao, H. Yang and Z. Lan, *Electrochim. Acta*, 2007, **52**, 5334–5338.
36 C. Ding, H. Zhang, X. Li, T. Liu and F. Xing, *J. Phys. Chem. Lett.*, 2013, **4**, 1281–1294.
37 P. J. Cappillino, H. D. Pratt, N. S. Hudak, N. C. Tomson, T. M. Anderson and M. R. Anstey, *Adv. Energy Mater.*, 2014, **4**, 1300566.
38 S. Gu, K. Gong, E. Z. Yan and Y. Yan, *Energy Environ. Sci.*, 2014, **7**, 2986–2998.
39 B. Dunn, H. Kamath and J. M. Tarascon, *Science*, 2011, **334**, 928–935.